Chapter 4
Scattering

4.1 General Observations About Scattering Processes

Scattering experiments are an important tool of nuclear and particle physics. They are used both to study details of the interactions between different particles and to obtain information about the internal structure of atomic nuclei and their constituents. These experiments will therefore be discussed at length in the following.

In a typical scattering experiment, the object to be studied (the *target*) is bombarded with a beam of particles with (mostly) well-defined energy. Occasionally, a reaction of the form

$$\mathrm{a} + \mathrm{b} \rightarrow \mathrm{c} + \mathrm{d}$$

between the projectile and the target occurs. Here, a and b denote the beam- and target particles, and c and d denote the products of the reaction. In inelastic reactions, the number of the reaction products may be larger than two. The rate, the energies and masses of the reaction products and their angles relative to the beam direction may be determined with suitable systems of detectors.

It is nowadays possible to produce beams of a broad variety of particles (electrons, protons, neutrons, heavy ions,...). The beam energies available vary between 10^{-3} eV for "cold" neutrons up to several 10^{12} eV for protons. It is even possible to produce beams of secondary particles which themselves have been produced in high energy reactions. Some such beams are very short-lived, such as muons, π- or K-mesons, or hyperons ($\Sigma^{\pm}$, Ξ^{-}, Ω^{-}).

Solid, liquid or gaseous targets may be used as scattering material or, in storage ring experiments, another beam of particles may serve as the target. Examples of this last are the electron-positron storage ring LEP (Large Electron Positron collider) at

B. Povh et al., *Particles and Nuclei*, Graduate Texts in Physics,
DOI 10.1007/978-3-662-46321-5_4

CERN[1] in Geneva (maximum beam energy $E_{e^+,e^-} = 104.6\,\text{GeV}$), the "Tevatron" proton-antiproton storage ring at the FNAL[2] in the USA ($E_{p,\bar{p}} = 980\,\text{GeV}$) and HERA (Hadron-Elektron-Ringanlage), the electron-proton storage ring at DESY[3] in Hamburg ($E_e = 27.6\,\text{GeV}$, $E_p = 920\,\text{GeV}$), which last was operated from 1992 to 2007, or the proton-proton storage ring LHC (Large Hadron Collider) at CERN with a nominal expected beam energy of $E_p = 7\,\text{TeV}$.

Figure 4.1 shows some scattering processes. We distinguish between elastic and inelastic scattering reactions.

Elastic scattering In an elastic process

$$a + b \rightarrow a' + b',$$

the same particles are present both before and after the scattering (Fig. 4.1a). The target b remains in its ground state, absorbing merely the recoil momentum and hence changing its kinetic energy. The apostrophe indicates that the particles in the initial and in the final state are identical up to momenta and energy. The scattering angle and the energy of the a′ particle and the production angle and energy of b′ are unambiguously correlated. As in optics, conclusions about the spatial shape of the

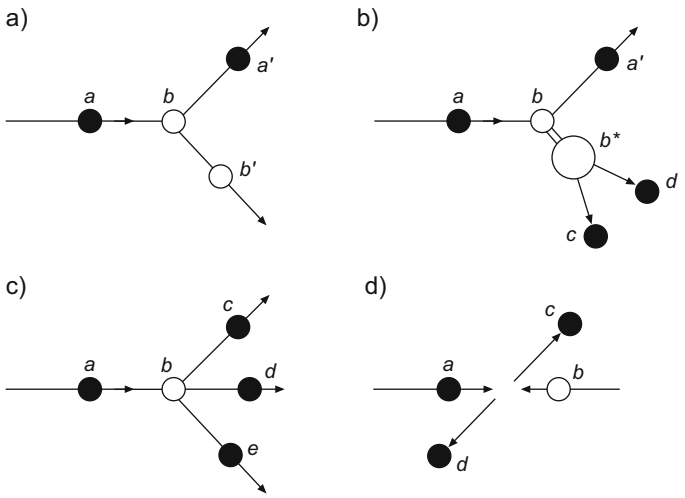

Fig. 4.1 Scattering processes: (**a**) elastic scattering; (**b**) inelastic scattering – production of an excited state which then decays into two particles; (**c**) inelastic production of new particles; (**d**) reaction of colliding beams

[1] Conseil Européen pour la Recherche Nucléaire.

[2] Fermi National Accelerator Laboratory.

[3] Deutsches Elektronen-Synchrotron.

scattering object can be drawn from the dependence of the scattering rate upon the beam energy and scattering angle.

It is easily seen that in order to resolve small target structures, larger beam energies are required. The reduced de Broglie wavelength $\lambda\!\!\!^{-} = \lambda/2\pi$ of a particle with momentum p is given by

$$\lambda\!\!\!^{-} = \frac{\hbar}{p} = \frac{\hbar c}{\sqrt{2mc^2 E_{\text{kin}} + E_{\text{kin}}^2}} \approx \begin{cases} \hbar/\sqrt{2mE_{\text{kin}}} & \text{for } E_{\text{kin}} \ll mc^2 \\ \hbar c/E_{\text{kin}} \approx \hbar c/E & \text{for } E_{\text{kin}} \gg mc^2 \,. \end{cases} \tag{4.1}$$

The largest wavelength that can resolve structures of linear extension Δx, is of the same order: $\lambda\!\!\!^{-} \lesssim \Delta x$.

From Heisenberg's uncertainty principle the corresponding particle momentum is:

$$p \gtrsim \frac{\hbar}{\Delta x} \,, \qquad pc \gtrsim \frac{\hbar c}{\Delta x} \approx \frac{200\,\text{MeV fm}}{\Delta x} \,. \tag{4.2}$$

Thus to study nuclei, whose radii are of a few fm, beam momenta of the order of 10–100 MeV/c are necessary. Individual nucleons have radii of about 0.8 fm; and may be resolved if the momenta are above $\approx$100 MeV/c. To resolve the constituents of a nucleon, the quarks, one has to penetrate deeply into the interior of the nucleon. For this purpose, beam momenta of many GeV/c are necessary (see Fig. 4.2).

Inelastic scattering In inelastic reactions

$$\begin{aligned} \mathrm{a} + \mathrm{b} &\to \mathrm{a}' + \mathrm{b}^* \\ &\quad\; \hookrightarrow \mathrm{c} + \mathrm{d} \,, \end{aligned}$$

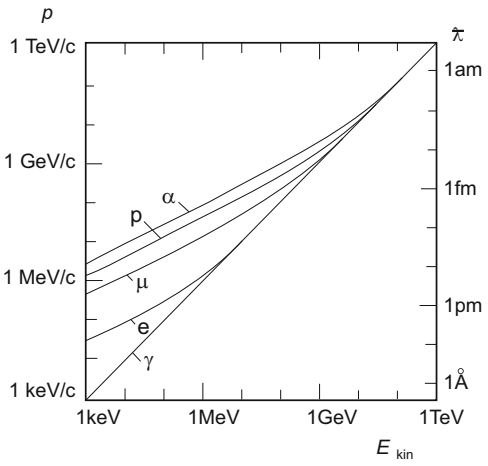

Fig. 4.2 The connection between kinetic energy, momentum and reduced wavelength of photons (γ), electrons (e), muons (μ), protons (p), and ^{4}He nuclei (α). Atomic diameters are typically a few Å (10^{-10} m), nuclear diameters a few fm (10^{-15} m)

part of the kinetic energy transferred from a to the target b excites it into a higher energy state b^* (Fig. 4.1b). The excited state will afterwards return to the ground state by emitting a light particle (e.g., a photon or a π-meson) or it may decay into two or more different particles.

A measurement of a reaction in which only the scattered particle a' is observed (and the other reaction products are not), is called an *inclusive* measurement. If all reaction products are detected, we speak of an *exclusive* measurement.

When allowed by the laws of conservation of lepton and baryon number (see Sects. 8.1 and 10.1), the beam particle may completely disappear in the reaction (Fig. 4.1c, d). Its total energy then goes into the excitation of the target or into the production of new particles. Such inelastic reactions represent the basis of nuclear and particle *spectroscopy,* which will be discussed in more detail in the second part of this book.

4.2 Cross-Sections

The reaction rates measured in scattering experiments, and the energy spectra and angular distributions of the reaction products yield, as we have already mentioned, information about the dynamics of the interaction between the projectile and the target, i.e., about the shape of the interaction potential and the coupling strength. The most important quantity for the description and interpretation of these reactions is the *cross-section* σ, which is a yardstick of the probability of a reaction between the two colliding particles.

Geometric reaction cross-section We consider an idealised experiment, in order to elucidate this concept. Imagine a thin scattering target of thickness d with N_b scattering centres b and with a particle density n_b. Each target particle has a cross-sectional area σ_b, to be determined by experiment. We bombard the target with a mono-energetic beam of point-like particles a. A reaction occurs whenever a beam particle hits a target particle, and we assume that the beam particle is then removed from the beam. We do not distinguish between the final target states, i.e., whether the reaction is elastic or inelastic. The total reaction rate $\dot{N}$, i.e., the total number of reactions per unit time, is given by the difference in the beam particle rate $\dot{N}_a$ upstream and downstream of the target. This is a direct measure for the cross-sectional area σ_b (Fig. 4.3).

We further assume that the beam has cross-sectional area A and particle density n_a. The number of projectiles hitting the target per unit area and per unit time is called the *flux* Φ_a. This is just the product of the particle density and the particle velocity v_a:

$$\Phi_a = \frac{\dot{N}_a}{A} = n_a \cdot v_a \,, \tag{4.3}$$

and has dimensions $[(\text{area} \times \text{time})^{-1}]$.

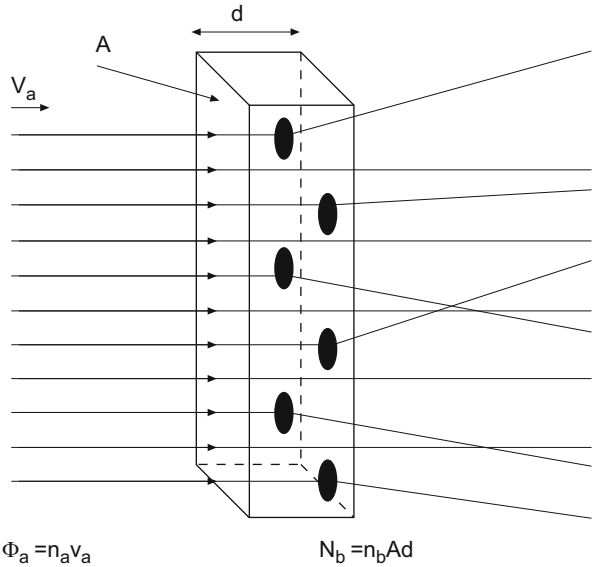

Fig. 4.3 Measurement of the geometric reaction cross-section. The particle beam, a, coming from the left with velocity v_a and density n_a, corresponds to a particle flux $\Phi_a = n_a v_a$. It hits a (macroscopic) target of thickness d and cross-sectional area A. Some beam particles are scattered by the scattering centres of the target, i.e., they are deflected from their original trajectory. The frequency of this process is a measure of the cross-sectional area of the scattering particles

The total number of target particles within the beam area is $N_b = n_b \cdot A \cdot d$. Hence the reaction rate $\dot{N}$ is given by the product of the incoming flux and the total cross-sectional area seen by the particles:

$$\dot{N} = \Phi_a \cdot N_b \cdot \sigma_b \,. \tag{4.4}$$

This formula is valid as long as the scattering centres do not overlap and particles are only scattered off individual scattering centres. The area presented by a single scattering centre to the incoming projectile a, will be called the *geometric reaction cross-section*: in what follows:

$$\begin{aligned} \sigma_b &= \frac{\dot{N}}{\Phi_a \cdot N_b} \\ &= \frac{\text{number of reactions per unit time}}{\text{beam particles per unit time per unit area} \times \text{scattering centres}} \,. \end{aligned} \tag{4.5}$$

This definition assumes a homogeneous, constant beam (e.g., neutrons from a reactor). In experiments with particle accelerators, the formula used is

$$\sigma_{\mathrm{b}} = \frac{\text{number of reactions per unit time}}{\text{beam particles per unit time} \times \text{scattering centres per unit area}} ,$$

since the beam is then generally not homogeneous but the area density of the scattering centres is.

Cross-sections This naive description of the geometric reaction cross-section as the effective cross-sectional area of the target particles, (if necessary convoluted with the cross-sectional area of the beam particles) is in many cases a good approximation to the true reaction cross-section. An example is high-energy proton-proton scattering where the geometric extent of the particles is comparable to their interaction range.

The reaction probability for two particles is, however, generally very different to what these geometric considerations would imply. Furthermore a strong energy dependence is also observed. The reaction rate for the capture of thermal neutrons by uranium, for example, varies by several orders of magnitude within a small energy range. The reaction rate for scattering of (point-like) neutrinos, which only feel the weak interaction, is much smaller than that for the scattering of (also point-like) electrons which feel the electromagnetic interaction.

The shape, strength and range of the interaction potential, and not the geometric forms involved in the scattering process, primarily determine the effective cross-sectional area. The interaction can be determined from the reaction rate if the flux of the incoming beam particles, and the area density of the scattering centres are known, just as in the model above. The *total cross-section* is defined analogously to the geometric one:

$$\sigma_{\mathrm{tot}} = \frac{\text{number of reactions per unit time}}{\text{beam particles per unit time} \times \text{scattering centres per unit area}} .$$

In analogy to the *total* cross-section, cross-sections for *elastic* reactions σ_{el} and for *inelastic* reactions σ_{inel} may also be defined. The inelastic part can be further divided into different reaction channels. The *total cross-section* is the sum of these parts:

$$\sigma_{\mathrm{tot}} = \sigma_{\mathrm{el}} + \sigma_{\mathrm{inel}} . \tag{4.6}$$

The cross-section is a physical quantity with dimensions of [area], and is independent of the specific experimental design. A commonly used unit is the *barn,* which is defined as

$$\begin{aligned} 1 \text{ barn} &= 1 \text{ b} = 10^{-28} \text{ m}^2 \\ 1 \text{ millibarn} &= 1 \text{ mb} = 10^{-31} \text{ m}^2 \\ &\text{etc.} \end{aligned}$$

Typical total cross-sections at a beam energy of 10 GeV, for example, are

$$\sigma_{\mathrm{pp}}(10\,\mathrm{GeV}) \approx 40\,\mathrm{mb} \tag{4.7}$$

for proton-proton scattering, and

$$\sigma_{\nu\mathrm{p}}(10\ \mathrm{GeV}) \approx 7 \cdot 10^{-14}\ \mathrm{b} = 70\ \mathrm{fb} \tag{4.8}$$

for neutrino-proton scattering.

Luminosity The quantity

$$\mathcal{L} = \Phi_{\mathrm{a}} \cdot N_{\mathrm{b}} \tag{4.9}$$

is called the *luminosity*. Like the flux, it has dimensions of $[(\mathrm{area}{\times}\mathrm{time})^{-1}]$. From (4.3) and $N_{\mathrm{b}} = n_{\mathrm{b}} \cdot d \cdot A$ we have

$$\mathcal{L} = \Phi_{\mathrm{a}} \cdot N_{\mathrm{b}} = \dot{N}_{\mathrm{a}} \cdot n_{\mathrm{b}} \cdot d = n_{\mathrm{a}} \cdot v_{\mathrm{a}} \cdot N_{\mathrm{b}}\ . \tag{4.10}$$

Hence the luminosity is the product of the number of incoming beam particles per unit time $\dot{N}_{\mathrm{a}}$, the target particle density in the scattering material n_{b}, and the target's thickness d; or the beam particle density n_{a}, their velocity v_{a} and the number of target particles N_{b} exposed to the beam.

There is an analogous equation for the case of two particle beams colliding in a storage ring. Assume that j particle packets, each of N_{a} or N_{b} particles, have been injected into a ring of circumference U. The two particle types circulate with velocity v in opposite directions. Steered by magnetic fields, they collide at an interaction point $j \cdot v/U$ times per unit time. The luminosity is then

$$\mathcal{L} = \frac{N_{\mathrm{a}} \cdot N_{\mathrm{b}} \cdot j \cdot v/U}{A}\,, \tag{4.11}$$

where A is the beam cross-section at the collision point. For a Gaussian distribution of the beam particles around the beam centre (with horizontal and vertical standard deviations σ_x and σ_y respectively), A is given by

$$A = 4\pi\sigma_x\sigma_y\,. \tag{4.12}$$

To achieve a high luminosity, the beams must be focused at the interaction point into the smallest possible cross-sectional area possible. Typical beam diameters are of the order of tenths of millimetres or less.

An often used quantity in storage ring experiments is the integrated luminosity $\int \mathcal{L}\,\mathrm{d}t$. The number of reactions which can be observed in a given reaction time is just the product of the integrated luminosity and the cross-section. With a 1 nb

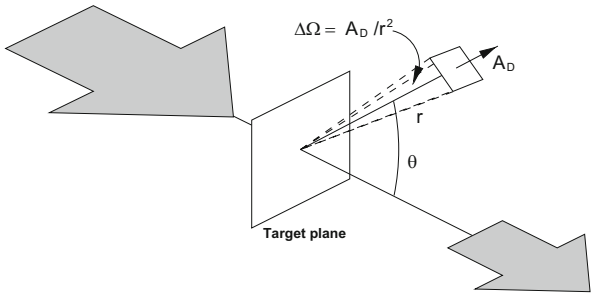

Fig. 4.4 Description of the differential cross-section. Only particles scattered into the small solid angle $\Delta\Omega$ are recorded by the detector of cross-sectional area A_D

cross-section and a $100\,\mathrm{pb}^{-1}$ integrated luminosity, for example, 10^5 reactions would be expected.

Differential cross-sections In practice, only a fraction of all the reactions are measured. A detector of area A_D is placed at a distance r and at an angle θ with respect to the beam direction, covering a solid angle $\Delta\Omega = A_\mathrm{D}/r^2$ (Fig. 4.4). The rate of reactions seen by this detector is then proportional to the *differential cross-section* $\mathrm{d}\sigma(E,\theta)/\mathrm{d}\Omega$:

$$\dot{N}(E,\theta,\Delta\Omega) = \mathcal{L}\cdot\frac{\mathrm{d}\sigma(E,\theta)}{\mathrm{d}\Omega}\Delta\Omega\ . \tag{4.13}$$

If the detector can determine the energy E' of the scattered particles then one can measure the *doubly differential* cross-section $\mathrm{d}^2\sigma(E,E',\theta)/\mathrm{d}\Omega\,\mathrm{d}E'$. The total cross-section σ is then the integral over the total solid angle and over all scattering energies:

$$\sigma_\mathrm{tot}(E) = \int_0^{E'_\mathrm{max}}\int_{4\pi}\frac{\mathrm{d}^2\sigma(E,E',\theta)}{\mathrm{d}\Omega\ \mathrm{d}E'}\,\mathrm{d}\Omega\ \mathrm{d}E'\ . \tag{4.14}$$

4.3 The "Golden Rule"

The cross-section can be experimentally determined from the reaction rate $\dot{N}$, as we saw above. We now outline how it may be found from theory.

First, the reaction rate is dependent upon the properties of the interaction potential described by the Hamilton operator $\mathcal{H}_\mathrm{int}$. In a reaction, this potential transforms the initial-state wave function ψ_i into the final-state wave function ψ_f. The *transition matrix element* is given by

$$\mathcal{M}_{fi} = \langle\psi_f|\mathcal{H}_\mathrm{int}|\psi_i\rangle = \int\psi_f^*\ \mathcal{H}_\mathrm{int}\ \psi_i\ \mathrm{d}V\ . \tag{4.15}$$

This matrix element is also called the *probability amplitude* for the transition.

Furthermore, the reaction rate will depend upon the number of final states available to the reaction. According to the uncertainty principle, each particle occupies a volume $h^3 = (2\pi\hbar)^3$ in *phase space*, the six-dimensional space of momentum and position. Consider a particle scattered into a volume V and into a momentum interval between p' and $p' + \mathrm{d}p'$. In momentum space, the interval corresponds to a spherical shell with inner radius p' and thickness $\mathrm{d}p'$ which has a volume $4\pi p'^2 \mathrm{d}p'$. Excluding processes where the spin changes, the number of final states available is

$$\mathrm{d}n(p') = \frac{V \cdot 4\pi p'^2}{(2\pi\hbar)^3} \mathrm{d}p' \,. \tag{4.16}$$

The energy and momentum of a particle are connected by

$$\mathrm{d}E' = v' \mathrm{d}p' \,. \tag{4.17}$$

Hence the density of final states in the energy interval $\mathrm{d}E'$ is given by

$$\varrho(E') = \frac{\mathrm{d}n(E')}{\mathrm{d}E'} = \frac{V \cdot 4\pi p'^2}{v' \cdot (2\pi\hbar)^3} \,. \tag{4.18}$$

The connection between the reaction rate, the transition matrix element and the density of final states is expressed by Fermi's *second golden rule*. Its derivation can be found in quantum mechanics textbooks (e.g. [2]). It expresses the reaction rate W per target particle and per beam particle in the form:

$$W = \frac{2\pi}{\hbar} \left|\mathcal{M}_{fi}\right|^2 \cdot \varrho(E') \,. \tag{4.19}$$

We also know, however, from (4.3) and (4.4) that

$$W = \frac{\dot{N}(E)}{N_\mathrm{b} \cdot N_\mathrm{a}} = \frac{\sigma \cdot v_\mathrm{a}}{V} \,, \tag{4.20}$$

where $V = N_\mathrm{a}/n_\mathrm{a}$ is the spatial volume occupied by the beam particles. Hence, the cross-section is

$$\sigma = \frac{2\pi}{\hbar \cdot v_\mathrm{a}} \left|\mathcal{M}_{fi}\right|^2 \cdot \varrho\,(E') \cdot V \,. \tag{4.21}$$

If the interaction potential is known, the cross-section can be calculated from (4.21). Otherwise, the cross-section data and Eq. (4.21) can be used to determine the transition matrix element.

The golden rule applies to both scattering and spectroscopic processes. Examples of the latter are the decay of unstable particles, excitation of particle resonances and transitions between different atomic or nuclear energy states. In these cases we have

$$W = \frac{1}{\tau} , \tag{4.22}$$

and the transition probability per unit time can be either directly determined by measuring the lifetime τ or indirectly read off from the energy width of the state $\Delta E = \hbar/\tau$.

4.4 Feynman Diagrams

> In QED, as in other quantum field theories, we can use the little pictures invented by my colleague Richard Feynman, which are supposed to give the illusion of understanding what is going on in quantum field theory.
>
> M. Gell-Mann [1]

Elementary processes such as the scattering of two particles off each other or the decay of a single particle are nowadays commonly depicted by *Feynman diagrams*. Originally, these diagrams were introduced by Feynman as a sort of shorthand for the individual terms in his calculations of transition matrix elements $\mathcal{M}_{fi}$ in electromagnetic processes in the framework of *quantum electrodynamics* (QED). Each symbol in such a space-time diagram corresponds to a term in the matrix element. The meaning of the individual terms and the links between them are fixed by the *Feynman rules*. Similarly to the QED rules, corresponding prescriptions exist for the calculation of weak and strong processes as well, in *quantum chromodynamics* (QCD). We will not use such diagrams for quantitative calculations, since this requires knowledge of relativistic field theory. Instead, they will serve as pictorial illustrations of the processes that occur. We will therefore merely treat a few examples below and explain some of the definitions and rules.

Figure 4.5 shows some typical diagrams. We use the convention that the time axis runs upwards and the space axis from left to right. The straight lines in the graphs correspond to the wave functions of the initial and final fermions. Antiparticles (in our examples: the positron e^+, the positive muon μ^+ and the electron-antineutrino $\overline{\nu}_e$) are symbolised by arrows pointing backwards in time; photons by wavy lines; heavy vector bosons by dashed lines; and gluons by corkscrew-like lines.

As we mentioned in Chap. 1, the electromagnetic interaction between charged particles proceeds via photon exchange. Figure 4.5a depicts schematically the elastic

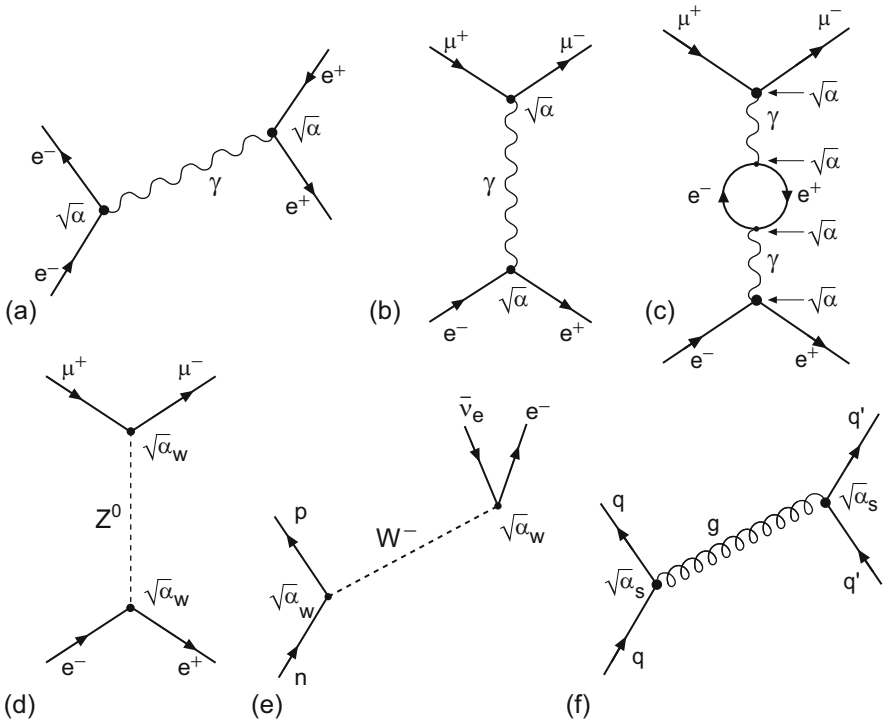

Fig. 4.5 Feynman diagrams for the electromagnetic (**a**–**c**), weak (**d**, **e**) and strong interactions (**f**)

scattering of an electron off a positron. The interaction process corresponds to a photon being emitted by the electron and absorbed by the positron. Particles appearing neither in the initial nor in the final state, such as this exchanged photon, are called *virtual particles*. Because of the uncertainty principle, virtual particles do not have to satisfy the energy-momentum relation $E^2 = \boldsymbol{p}^2c^2 + m^2c^4$. This may be interpreted as meaning that the exchanged particle has a mass different from that of a free (real) particle, or that energy conservation is violated for a brief period of time.

Points at which three or more particles meet are called *vertices.* Each vertex corresponds to a term in the transition matrix element which includes the structure and strength of the interaction. In (a), the exchanged photon couples to the charge of the electron at the left vertex and to that of the positron at the right vertex. For each vertex the transition amplitude contains a factor which is proportional to e, i.e., $\sqrt{\alpha}$.

Figure 4.5b represents the annihilation of an electron-positron pair. A photon is created as an intermediate state which then decays into a negatively charged μ^- and its positively charged antiparticle, a μ^+. Figure 4.5c shows a slightly more complicated version of the same process. Here, the photon, by vacuum polarisation, is briefly transformed into an intermediate state made up of an e^+e^- pair. This and

additional, more complicated, diagrams contributing to the same process are called *higher-order diagrams*.

The transition matrix element includes the superposition of amplitudes of all diagrams leading to the same final state. Because the number of vertices is greater in higher-order diagrams these graphs include higher powers of α. The amplitude of diagram (b) is proportional to α, while diagram (c)'s is proportional to α^2. The cross-section for conversion of an electron-positron pair into a $\mu^+\mu^-$ pair is therefore given to a good approximation by diagram (b). Diagram (c) and other diagrams of even higher order produce only small corrections to (b).

Figure 4.5d shows electron-positron annihilation followed by muon pair production in a weak interaction proceeding through exchange of the neutral, heavy vector boson Z^0. In Fig. 4.5e, we see a neutron transform into a proton via β-decay in which it emits a negatively charged heavy vector boson W^- which subsequently decays into an electron and antineutrino $\overline{\nu}_e$. Figure 4.5f depicts a strong interaction process between two quarks q and q′ which exchange a gluon, the field quantum of the strong interaction.

In weak interactions, a heavy vector boson is exchanged which couples to the "weak charge" g and not to the electric charge e. Accordingly, $\mathcal{M}_{fi} \propto g^2 \propto \alpha_w$. In strong interactions the gluons which are exchanged between the quarks couple to the "colour charge" of the quarks, $\mathcal{M}_{fi} \propto \sqrt{\alpha_s} \cdot \sqrt{\alpha_s} = \alpha_s$.

The exchange particles contribute a *propagator* term to the transition matrix element. This contribution has the general form

$$\frac{1}{Q^2 + M^2c^2} \,. \tag{4.23}$$

Here Q^2 is the square of the four-momentum (cf. (5.3) and (6.3)) which is transferred in the interaction and M is the mass of the exchange particle. In the case of a virtual photon, this results in a factor $1/Q^2$ in the amplitude and $1/Q^4$ in the cross-section. In the weak interaction, the large mass of the exchanged vector boson causes the cross-section to be much smaller than that of the electromagnetic interaction – although at very high momentum transfers, of the order of the masses of the vector bosons, the two cross-sections become comparable in size, as it has been demonstrated at the electron-proton storage ring HERA (cf. Sect. 12.2).

Problems

1. **Cross-section**
   Deuterons with an energy $E_{kin} = 5\,\text{MeV}$ are perpendicularly incident upon a tritium target, which has a mass occupation density $\mu_t = 0.2\,\text{mg/cm}^2$, so as to investigate the reaction $^3\text{H(d, n)}^4\text{He}$.

(a) How many neutrons per second pass through a detector with a reception area of $A = 20\,\mathrm{cm}^2$ which is at a distance $R = 3\,\mathrm{m}$ from the target and an angle $\theta = 30°$ to the deuteron beam direction, if the differential cross-section $\mathrm{d}\sigma/\mathrm{d}\Omega$ at this angle is 13 mb/sr and the deuteron current applied to the target is $I_\mathrm{d} = 2\,\mu\mathrm{A}$?
(b) How many neutrons per second does the detector receive if the target is tilted so that the same deuteron current now approaches it at 80° instead of 90°?

2. **Absorption length**
A particle beam is incident upon a thick layer of an absorbing material (with n absorbing particles per unit volume). How large is the absorption length, i.e., the distance over which the intensity of the beam is reduced by a factor of $1/\mathrm{e}$ for the following examples?

(a) Thermal neutrons ($E \approx 25\,\mathrm{meV}$) in cadmium ($\varrho = 8.6\,\mathrm{g/cm}^3$, $\sigma = 24\,506\,\mathrm{barn}$).
(b) $E_\gamma = 2\,\mathrm{MeV}$ photons in lead ($\varrho = 11.3\,\mathrm{g/cm}^3, \sigma = 15.7$ barn/atom).
(c) Antineutrinos from a reactor in earth ($\varrho = 5\,\mathrm{g/cm}^3$, $\sigma \approx 10^{-19}$ barn/electron; interactions with nuclei may be neglected; $Z/A \approx 0.5$).

References

1. M. Gell-Mann, in *The Nature of Matter*, ed. by J.H. Mulvey. Wolfson College Lectures (Clarendon Press, Oxford, 1980)
2. F. Schwabl, *Quantum Mechanics*, 4th edn. (Springer, Berlin/Heidelberg/New York, 2007)